



IntelliLining: Activity Sensing through Textile Interlining Sensors Using TENGs

Mahdie Ghane Ezabadi

Computing Science

Simon Fraser University

Burnaby, British Columbia, Canada

mahdie_ghane@sfu.ca

Xing-Dong Yang

School of Computing Science

Simon Fraser University

Burnaby, British Columbia, Canada

xingdong_yang@sfu.ca

Aditya Shekhar Nittala

Department of Computer Science

University of Calgary

Calgary, Alberta, Canada

anittala@ucalgary.ca

Te-Yen Wu

Computer Science

Florida State University

Tallahassee, Florida, USA

twu@cs.fsu.edu

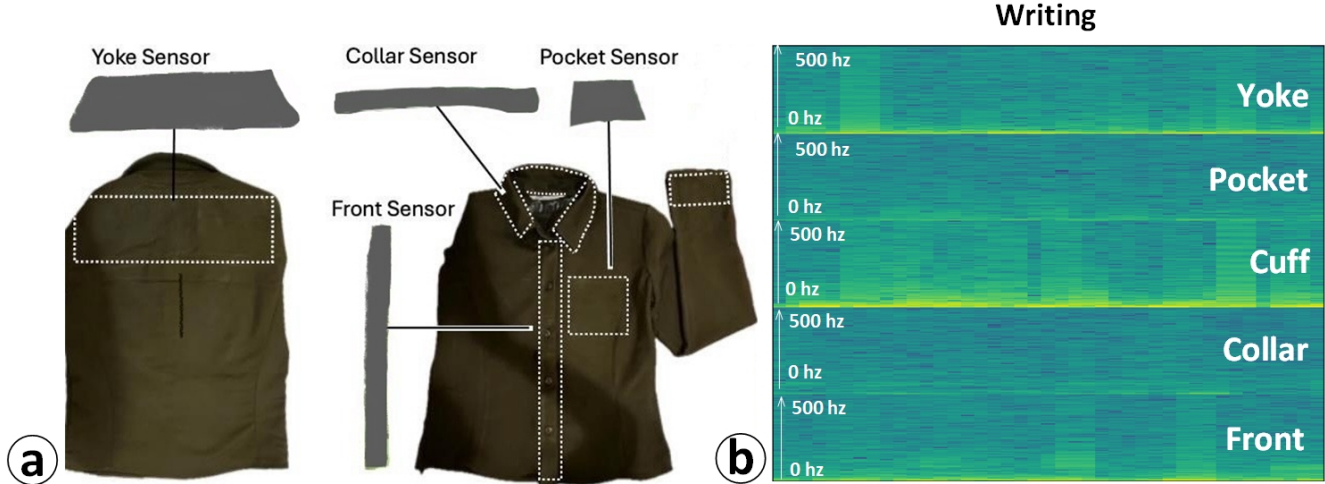


Figure 1: (a) Illustration of smart interlinings (gray), which serve as a new form of interactive garment component designed to sense user activities through vibration sensing. (b) Captured signals from various smart interlining sensors while the user was engaged in writing.

Abstract

We introduce a novel component for smart garments: smart interlining, and validate its technical feasibility through a series of experiments. Our work involved the implementation of a prototype that employs a textile vibration sensor based on Triboelectric Nanogenerators (TENGs), commonly used for activity detection. We explore several unique features of smart interlining, including

how sensor signals and patterns are influenced by factors such as the size and shape of the interlining sensor, the location of the vibration source within the sensor area, and various propagation media, such as airborne and surface vibrations. We present our study results and discuss how these findings support the feasibility of smart interlining. Additionally, we demonstrate that smart interlinings on a shirt can detect a variety of user activities involving the hand, mouth, and upper body, achieving an accuracy rate of 93.9% in the tested activities.

Permission to make digital or hard copies of all or part of this work for personal or classroom use is granted without fee provided that copies are not made or distributed for profit or commercial advantage and that copies bear this notice and the full citation on the first page. Copyrights for components of this work owned by others than the author(s) must be honored. Abstracting with credit is permitted. To copy otherwise, or republish, to post on servers or to redistribute to lists, requires prior specific permission and/or a fee. Request permissions from permissions@acm.org.

CHI '25, Yokohama, Japan

© 2025 Copyright held by the owner/author(s). Publication rights licensed to ACM.

ACM ISBN 979-8-4007-1394-1/25/04

<https://doi.org/10.1145/3706598.3713167>

CCS Concepts

- Human-centered computing → Ubiquitous and mobile computing systems and tools; • Human-computer interaction; • Smart textile; • Textile microphone;

Keywords

Interactive textile, TENGs, Machine learning, Vibration sensing

ACM Reference Format:

Mahdie Ghane Ezabadi, Aditya Shekhar Nittala, Xing-Dong Yang, and Te-Yen Wu. 2025. IntelliLining: Activity Sensing through Textile Interlining Sensors Using TENGs. In *CHI Conference on Human Factors in Computing Systems (CHI '25), April 26–May 01, 2025, Yokohama, Japan*. ACM, New York, NY, USA, 14 pages. <https://doi.org/10.1145/3706598.3713167>

1 Introduction

Sensor-powered smart garments can collect daily activity data, such as eating habits and fitness routines, enabling numerous new applications in health, wellness, and safety [8, 21–23, 28, 52, 54]. Traditionally, sensors are added to garments as ‘aftermarket’ attachments, which, while functional, do not merge seamlessly into the garments. Recent research has, therefore, focused on embedding sensors directly into garment components, including rigid elements, such as buttons [11] or zippers [24], and soft elements, such as drawstrings [31, 39], seams [37, 49], and pockets [44]. This approach could significantly improve aesthetics, comfort, and integration with existing garment production processes.

In this paper, we extend this body of research to a new soft garment component—interlining, a commonly used element in garments such as shirts, jackets, and coats. Interlining provides reinforcement in areas like the collar and cuff, ensuring their intended shape is maintained during body movements [53]. In contrast to existing soft smart garment components, such as seams [37, 49] or drawstrings [31, 39], interlining offers a 2D surface area, making it suitable for a wider range of sensing techniques. This is particularly useful for exploring the full potential of smart garments. Furthermore, the distributed placement of interlinings throughout a garment also enables multiple alternative sensing channels, enabling the detection of a wider range of activities, such as the hands (e.g., via the interlining at the sleeve cuff), upper body (e.g., via the interlining at the yoke or chest), mouth (e.g., via the interlining at the collar), as well as their combinations.

We explore the technical feasibility of smart interlinings by employing a textile sensing technique commonly used for activity detection: vibration sensors based on the Triboelectric Nanogenerators (TENG) effect [39, 45]. While TENG sensors have proven effective in body-worn items, such as sleeves [21] and gloves [45], for monitoring body movement, research on their applicability to interlinings is limited. For example, TENG sensors can detect limb movement when attached to joints [14]. However, this capability does not directly translate to smart interlinings, which are typically not located in areas that experience significant bending during user activities. Consequently, questions remain about how sensor signals and patterns respond to daily activities, considering factors unique to interlinings, like varying sizes and shapes within a garment (e.g., flat on a chest pocket versus circular on a sleeve cuff), varying location of the vibration source within a sensor area, and differing propagation media such as airborne and surface vibrations. Understanding these aspects is crucial for developing a functional system.

To address this, we developed several TENG-based prototypes (called IntelliLining) matching the shape and size of typical shirt

interlinings, including the sleeve cuff, front placket, yoke (shoulder), chest pocket, and collar. Through experiments, we report how the aforementioned factors influence sensor signals.

Further, to demonstrate the unique capability of smart interlining in detecting a diverse range of activities involving various body parts, we conducted an experiment using IntelliLining integrated into a shirt. We selected twelve activities across three categories: hand-based activities (e.g., wiping a desk), mouth-based activities (e.g., speaking), and activities that combine the use of the mouth, hands, and often upper body movements (e.g., eating and walking). Our results showed that recognition accuracy exceeded 90% under many conditions. While previous studies have used soft textile sensors to detect a certain category of activities, such as those involving the arm, IntelliLining is the first smart garment component to sense such a broad array of activities.

The key contributions of this work are: (1) Introducing the novel concept of smart interlining. (2) Presenting findings from technical experiments that offer insights into the feasibility of IntelliLining. (3) Demonstrating through an experiment that a shirt equipped with smart interlining can detect a diverse range of daily activities.

2 Background and Related Work

In this section, we review previous research on sensor-powered garments, emphasizing the different approaches for incorporating sensors into garments: the ‘aftermarket’ approach versus converting garment components into sensors. Additionally, we will discuss existing work on activity recognition using textile TENG.

2.1 Sensors as "Aftermarket" Attachments

Most existing work demonstrating new sensing capabilities involves incorporating soft or textile sensors into garments as “aftermarket” attachments, added to a finished garment. This approach is useful for rapid prototyping, providing greater flexibility in sensor placement. For instance, sensors can be strategically positioned near key sources of body movement, such as joints, to enhance signal clarity. Examples include the attachment of soft sensors along the arm [8, 21, 27, 29, 48], shoulder [8, 23, 27], chest [8, 12], torso [27, 29], waist[27], and fingers[40, 45, 48] where body movements are most effectively captured.

For instance, in MoCapaci [8], thread sensors were attached to locations such as the chest, shoulder, and arm of an off-the-shelf garment. This implementation enabled the detection of up to 20 body posture gestures without alerting the garment’s original structure. Similarly, other research, including those by Koyama et al. [23] and Lin et al. [27], attached sensors to off-the-shelf garments at various locations like the shoulder, arm, torso, and waist. These projects focused on recognizing both static postures and dynamic activities, such as eating, walking, toothbrushing, running, and jumping.

It is important to note that these works primarily aimed to demonstrate sensing capabilities and facilitate rapid prototyping. As a result, the sensors employed, often rigid in design, were not intended for seamless integration into garments, often compromising both aesthetics and comfort. In contrast, our work seeks to address this challenge by incorporating sensing capabilities into garment components. The novelty of our work lies in the selection

of interlinings, which allow for the distributed placement of sensors across various garment areas (e.g., sleeve cuff, front placket, yoke (shoulder), chest pocket, and collar), thus broadening the range of activities that smart garment components can detect.

2.2 Smart Garment Components

Recent advances in sensor-powered garments are increasingly focused on transforming traditional garment components into smart elements with integrated sensing capabilities for activity recognition. This approach holds promise for seamlessly embedding sensors into garments, thereby enhancing aesthetics, comfort, and compatibility with existing garment production processes. Researchers have explored a range of garment components for these applications, including rigid components such as buttons [11] or zippers [24], as well as soft components, like drawstrings [31], seams [37, 49], sleeves [33], and pockets [44].

For example, Zippro [24] is a smart zipper embedded with infrared (IR), fingerprint, and capacitive sensors, enabling it to detect a range of explicit user inputs such as taps, swipes, and different grip types, as well as to recognize users by their fingerprints. Similarly, Sensorsmap [11] transforms ordinary buttons into smart components capable of recognizing touch and gestures through embedded an IMU sensor.

In addition to rigid garment components, soft components also present significant potential for sensing user input or activities. For instance, Serpentine [31], a smart drawstring based on TENG, can detect various finger gestures such as pinching, twirling, plucking, stretching, twisting, and wiggling. Similarly, Smartsleeve [33] transforms a sleeve into a sensor for arm movements, utilizing piezoelectric fabric to detect different arm postures based on surface deformation.

An essential component of garments is the seam, which can be found in various locations on clothing. Recent research has explored the potential of converting seams into sensors for detecting user activities. For instance, in [37], seams along the sleeve were used to detect 12 different activities involving arm movements. Another study [49] utilized seams on the back, front, and collar to predict joint positions. Moreover, pockets have been enhanced for sensing purposes, as demonstrated in Tesca [44], where pockets were used to detect various objects people carry, such as keys and AirPods.

This body of research offers promising opportunities for the future development of sensor-powered garments. However, several challenges remain. A key issue is that sensor placement is often restricted to specific locations within traditional garment components, which may not always be optimal for accurate activity sensing. This is particularly relevant for interlinings. Our work explores the feasibility of incorporating sensing capabilities into interlinings. Additionally, while most prior research has utilized soft sensors or smart garment components to detect specific types of activities, such as those involving arm movements, IntelliLining represents the first smart garment component capable of recognizing a broader range of activities.

2.3 Activity Recognition Using TENG

To achieve activity recognition on wearable devices, various sensor modalities have been used, including vibrations [9, 17, 20, 25, 52],

deformations [27, 30, 37], acceleration [20, 25], and pressure [19, 36, 40, 42]. Vibration sensors are particularly promising, as they can detect mechanical vibrations and, in some cases, near-range sounds [14]. This allows for the detection of activities involving the mouth, hand, and upper body movements, which are difficult to capture with a single sensor. Among vibration sensors, TENGs (Triboelectric Nanogenerators) [14] are well-suited for integration into garments, as they can be made from soft, fabric-based materials. TENGs detect vibrations through the triboelectric effect. When two materials with different electron affinities come into contact, electrons are transferred, creating a charge imbalance. As the materials separate, a potential difference is generated, driving current through an external circuit. This current is proportional to the separation distance, making TENGs highly sensitive to vibrations and capable of detecting dynamic movements such as hand, mouth, or upper body activities.

Researchers have investigated various methods to incorporate TENG sensors into clothing to detect simple body movements. For instance, TENG sensors have been integrated into shoes [26, 41, 46, 47], gloves [45], and pants [18, 51] to detect leg or knee movements, as well as into shirts to detect movements of the waists [52], and upper body [21, 39].

In work involving pants, TENG sensors have been affixed to joints, such as the knees, to monitor leg movements involving bending. Additionally, TENG sensors have been positioned near the calf to detect various activities, including sitting, walking, stair ascent and descent, and running [18]. Similarly, Zeng et al. [51] developed deformable TENG sensors for placement on the knee to identify activities such as walking, high jumps, high knee lifts, and slight jumps. In the context of shirts, TENG sensors have been used to detect upper body movements. For example, the work by Kiaghadi et al. [21] introduced a textile-based TENG affixed to the arm to identify a limited range of hand movements, such as toothbrushing, eating, and walking. Our work is different in that we validate the technical feasibility of smart interlinings implemented using TENG.

In contrast to previous approaches, our work focuses on investigating the feasibility of detecting user activities in areas conventionally reinforced with interlining. Although these locations may not offer the best conditions for capturing reliable sensor data, they are situated near the optimal sites highlighted in previous studies on the positioning of rigid wearable devices [16, 50]. Considering that many user activities produce vibrations propagated through surfaces or the air, we opted to incorporate vibration sensors in our implementation.

3 IntelliLining

This section presents the implementation of the IntelliLining sensor, its integration into a shirt, and an overview of the sensing capabilities it enables.

3.1 Sensor Fabrication

We fabricated the TENG sensor by placing a polytetrafluoroethylene (PTFE) film [4] between two layers of conductive fabric [5] (Figure 2a). The PTFE film functions as the negative triboelectric layer, while the conductive fabric layers serve both as electrodes and

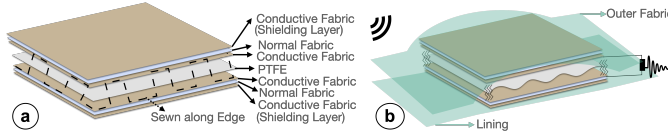


Figure 2: (a) An illustration of the sensor layers in our smart interlining implementation based on TENG. (b) An illustration of the smart interlining integrated between the fabric layers of a garment (shown in green).



Figure 3: Fabrication process of IntelliLining. (a) PTFE film is sandwiched between two layers of conductive fabric (b) and is sewn along the edges to create the sensor. (c) Regular fabric is ironed onto the sensor using fusible interfacing layer. (d) A shielding layer is added on both sides of the sandwich to minimize electromagnetic interference. (e) Finished IntelliLining. (f) IntelliLining is then integrated onto the shirt cuff (g) Ironing the interlining inside the cuff to bond it to the shirt fabric using heat-activated glue. (h) Resulting shirt with integrated IntelliLining.

as the positive triboelectric layer. The conductive fabric layers were attached to a non-conductive fabric substrate using iron-on fusible interfacing. The PTFE layer was sewn along the sensor's edge, rather than within the sensing area, which, according to our preliminary test, resulted in stronger signals due to greater movement space for the PTFE layer.

The IntelliLining prototype consists of the TENG sensor sandwiched between two layers of conductive fabric, which are attached to each side of the TENG surface using iron-on adhesive. These conductive fabric layers are electrically connected with conductive threads to provide shielding and minimize electromagnetic interference. The fully assembled smart interlining sensor has a thickness of around 1.5 mm and can be adhered between the fabric layers of a shirt, replacing its traditional non-smart equivalent (Figure 2b)

Interlinings are typically positioned in garments at locations such as the sleeve cuff, front placket, yoke (shoulder), chest pocket, and collar. We created prototypes for these interlinings based on the dimensions of a medium-sized women's shirt (see Figure 1). Although the size of interlinings (and consequently the sensors) varies with garment size, our study (Section 4) found that this variation does not significantly affect sensor signals. Additionally,

previous research [6] suggested that sensor geometry variations within our operational frequency range have negligible impact on the signal. Thus, we standardized our smart interlinings to rectangular shapes for simplicity, with dimensions as follows: sleeve cuff: $22.9\text{cm} \times 6.3\text{cm}$, front placket: $29.5\text{cm} \times 7.5\text{cm}$, yoke: $46.3\text{cm} \times 15\text{cm}$, chest pocket: $12\text{cm} \times 12\text{cm}$, and collar: $42.5\text{cm} \times 2.5\text{cm}$.

3.2 Integration into a Shirt

Upon completion, the IntelliLining need to be integrated into a shirt, replacing the original interlinings (Figure 1). To assess the ease of installation, we evaluated our prototype with users experienced in interlining and sewing. We invited two sewers, each with several years of experience, to install the IntelliLining into a women's shirt, following the standard workflow. Specifically, they were instructed to attach the IntelliLining using iron-on fusible interfacing, a standard method for securing interlinings to shirts [53]. Both sewers completed the task within an hour. They noted that, aside from the prototype being thicker than traditional interlinings, there was little difference, and the interlinings were easy to work with using standard tools while following the established workflow. Our initial tests confirmed that the sensors retained their functionality even after exposure to heat during the fabrication process.

3.3 Electronics

After the IntelliLining were installed, we connected each one to an ADC (we used Analog Discovery 2 [1] for the purpose) for data collection, with all electronic wires sewn to the shirt to minimize noise. Sensor data was sampled at 1kHz and transmitted to a laptop for processing via USB cables. The current setup is relatively bulky, requiring five separate ADCs. However, this configuration serves us well for testing the concept of smart interlinings. We anticipate that future developments could integrate the data collection, communication, and basic computation into a more compact unit, potentially leveraging higher-fidelity prototyping tools like Brookdale [38]. Ultimately, the electronics and battery system could be miniaturized to the size of a USB key, similar to Google's Jackarad [35].

3.4 What Can Be Sensed?

IntelliLining detects subtle vibrations from two primary sources: near-range airborne and surface vibrations. Airborne vibrations, such as those from speaking or coughing, travel through the air and are captured by the sensor. Since IntelliLining is securely affixed to the fabric of the shirt using adhesive, these vibrations propagate through the fabric layers to reach the sensor (see Section 4.1.4 for supporting evidence).

IntelliLining can also capture surface vibrations from body movements, which originate from sources such as clothing deformation. Many user activities generate both types of vibrations. For instance, chopping on a cutting board produces mechanical surface vibrations from the chopping motion and airborne vibrations from the sound of chopping. IntelliLining captures these vibrations at different locations of the garment. For instance, coughing sounds are best captured at the collar, while body or arm movements during coughing are more effectively detected at the yoke (shoulder) or sleeve cuff. By combining the data from this sensor network or a

subset of the sensors within the network, IntelliLining can identify a broader range of activities compared to single-point sensing.

3.5 IntelliLining Applications

IntelliLining can detect several different categories of activities through the smart interlinings embedded in various areas of the shirt. While previous research has used soft sensors or smart garment components to detect a certain category of activities, such as those involving banding arms [21], IntelliLining is the first smart garment component to recognize a broader range of activities. These include (1) hand-based activities, (2) mouth-based activities, and (3) activities involving combined use of the mouth, hands, and often upper body movements. The selection of these activities highlights IntelliLining's capabilities and reflects activities commonly explored in existing research, which typically rely on rigid or non-garment-based sensing devices [8, 23, 27, 32].

3.5.1 Activities involving the mouth. Activities involving sounds produced by the mouth can be primarily sensed through airborne vibrations. For example, when IntelliLining is placed near the mouth, such as in a collar, it can detect actions like coughing or snoring and monitor their frequency. This capability allows tracking of daily occurrences and durations, potentially aiding in recovery planning and predicting progress.

3.5.2 Activities involving the hand. When placed near the hand, such as in a sleeve cuff, IntelliLining captures surface and occasionally airborne vibrations produced by hand-related activities, such as writing or performing kitchen tasks like chopping or wiping (Figure 4). This data provides insights for skill development and self-reflection to help users identify areas for improvement.

3.5.3 Activities involving mouth, hand, and other body parts. This category includes activities that engage multiple body parts. For example, routine activities like eating, drinking, or coughing into a hand involve both the mouth and hand (Figure 4). By combining collar and sleeve cuff data, these activities can be better distinguished from those involving only the mouth, like speaking. Similarly, activities such as walking and tabletop crunches engage the entire upper body, including the arms, back, chest, and hands. Sensor data from locations like the sleeve cuff, chest pocket, and yoke collectively contribute to the accurate recognition of these activities, supporting health applications such as automated diet tracking.



Figure 4: Example of applications that involve hands or hands and mouth. The location of the potential interlining sensor is shown in red.

4 Experiments: Characterizing sensor signals

Understanding raw signal data is crucial for assessing IntelliLining's feasibility. Within the proposed usage scenarios, several factors may impact the TENG sensor's signals and signal patterns. For instance,

the interlinings in garments vary in size, potentially causing different signal responses to vibrations at different frequencies or even at the same frequency. Additionally, for sensors covering a relatively large area, the projected location of the vibration source within the sensor may also affect its signals. This variability poses challenges in accurately distinguishing between different activities. Moreover, interlining sensors cannot always maintain a flat configuration. Sensors placed on the sleeve cuff or collar, for instance, require bending into a cylinder shape, leading to increased tension within the sensor layers and potentially reducing sensitivity. Further, IntelliLining must detect both airborne and surface vibrations. Given the substantial differences in the size of the sensing area among the interlining at different locations, it remains uncertain whether consistently clear signals from both sources can be reliably captured. To address these issues and validate the feasibility of IntelliLining, we conducted a series of experiments to characterize the signals of interlining sensors.

4.1 Effect of Sensor Area Size

The primary goal of this experiment was to explore the potential influence of sensing area size on sensor signals across a broad range of vibration frequencies encountered in everyday activities.

4.1.1 Apparatus. We developed four IntelliLining sensors (Figure 5a) with areas ranging from 100 cm^2 to 700 cm^2 , incrementing in steps of 200 cm^2 . The interval between the largest and smallest sizes was equally divided, resulting in four interlinings with areas of 100 cm^2 , 300 cm^2 , 500 cm^2 , and 700 cm^2 . The 100cm^2 and 700cm^2 conditions were specifically chosen to represent the smallest (collar) and largest (yoke) interlinings of a medium-sized women's shirt.

The dimensions of the tested sensors are as follows: $40\text{cm} \times 2.5\text{cm}$, $30\text{cm} \times 10\text{cm}$, $25\text{cm} \times 20\text{cm}$, and $46.6\text{cm} \times 15\text{cm}$, for each respective size condition. To ensure the reliability of our findings, we created two prototypes for each size condition. Subsequently, we analyzed our results using the average of the data collected from the two copies. This approach was adopted to mitigate any potential impact on the findings stemming from inconsistencies in the fabrication process.

During the experiment, the sensors were placed on the back of a mannequin to replicate the uneven surface of the human body. The sensor surface was covered with fabric substrate on the inner side to mimic their placement within a garment. To better simulate the softness of the skin surface and the resulting sensor deformation, the back of the mannequin was covered with artificial skin. The mannequin was used instead of human participants to maintain a controlled experimental environment, as human participants could introduce uncontrolled variables, such as involuntary movements, that might compromise the reliability of the sensor performance measurements.

To produce a wide range of vibration frequencies, we utilized a speaker (Dayton DAEX25 [2]), which exhibits a consistent frequency response from 2 Hz to 2 kHz. This speaker was affixed to a concrete wall at approximately the same height as the center of the sensor, maintaining a distance of 15cm from the sensor. This setup is to simulate the scenarios in which the vibration signals travel through the air to the sensor, such as the case of a sensor integrated into a collar capturing coughing sound.

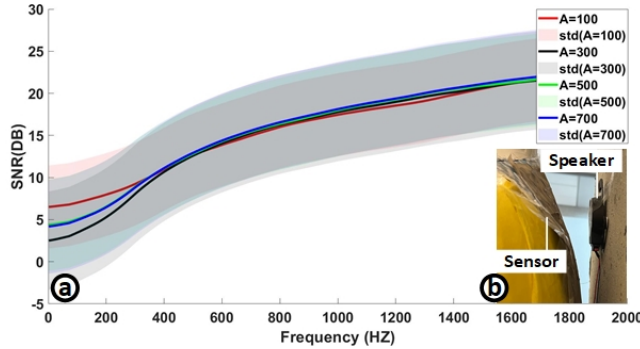


Figure 5: Experiment setup and results for effects of sensor area size on sensor’s sensitivity. (a) Experiment results. Comparison of sensor activity across different sizes. (b) During the experiment, the sensor was placed on the back of a mannequin 15 cm from the speaker.

4.1.2 Data Collection. During the experiment, the speaker was controlled using Analog Discovery 2 [1] to sweep frequencies ranging from 2Hz to 2kHz, with an incremental step size of 2Hz (Figure 5). This frequency range was purposefully chosen to include the usual frequencies of human speech [7] and everyday user activities [25]. The average output volume of the speaker was 68 dB, with measurements taken using a smartphone placed 15 cm from the speaker running the Decible X app. This specific volume and distance were chosen to simulate the case of a collar sensor capturing the human voice from the mouth. During the experiment, the speaker was controlled using Analog Discovery-2 [1] to sweep frequencies ranging from 2Hz to 2kHz, with an incremental step size of 2Hz (Figure 5). This frequency range was purposefully chosen to include the usual frequencies of human speech [7] and everyday user activities [25].

For every tested frequency, 10 samples were collected, resulting in a total of 10,000 data points for each replicated sensor of a specific size. Subsequently, the sensor signals received for each tested frequency were averaged for data analysis. To calculate the Signal-to-Noise Ratio (SNR), environmental noise data was collected using the same method but without the use of the speaker.

4.1.3 Result. The results for the effect of sensor area sizes are presented in Figure 5c. One-way Anova revealed no significant differences across four tested sensor areas ($F_{3,3996} = 1.7967$ and $P=0.1455$). This result suggests that the sensitivity of the IntelliLining sensor remains consistent regardless of the variation in interlining type. Moreover, it implies that sensor geometry, including variations in width-to-height ratios across the tested sensors, has a negligible influence on the sensor signal across different frequencies.

Furthermore, based on the Inverse Square Law and with a human speech frequency of approximately 200 Hz, it can be estimated that the sensor’s ability to detect human voices, a prevalent form of environmental noise, diminishes significantly beyond a distance of 30cm. This characteristic is advantageous in our application scenarios, as a close-range sensor effectively reduces the potential for capturing environmental noises, thereby enhancing the robustness of the system.

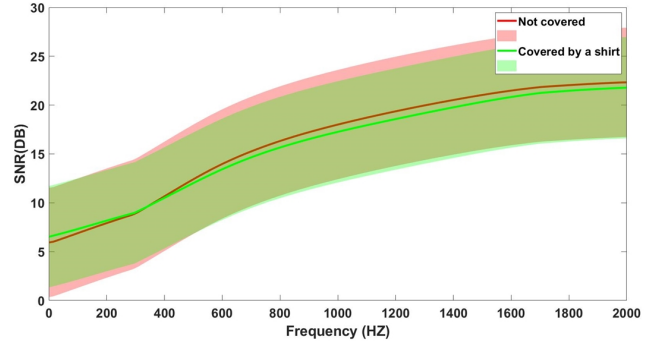


Figure 6: The sensor signals collected with and without the IntelliLining integrated into the shirt do not show any significant difference.

4.1.4 Effect of the sensor covered by the shirt. Note that our experiment was conducted without integrating the IntelliLining sensor into the shirt. To examine the potential impact of the shirt fabric on the sensor’s signal, we performed an additional test with the IntelliLining sensor integrated into the shirt using the method described in Section 3.2. As our results indicated no significant effect of the sensor’s area size on its signal, we only tested the larger sensor with an area of 700, cm^2 , positioned on the yoke. All other experimental settings remained unchanged. The results are shown in Figure 6. A one-way ANOVA revealed no significant differences between the two conditions ($F_{1,1998} = 3.422$, $p = 0.065$). This finding suggests that integrating the IntelliLining sensor into a shirt does not significantly affect its sensitivity. Therefore, for simplicity, subsequent experiments were conducted without integrating the sensor into the shirt.

4.2 Effect of Source Location within the Sensor

The objective of this study was to assess the sensitivity of the IntelliLining sensor in detecting vibrations transmitted through different locations within the sensor. Our focus was on investigating the influence of the vibration source’s location, whether it was positioned near the center or the edge of the sensor, on the sensor signals.

4.2.1 Apparatus. The experimental setup was similar to the previous study on sensor areas . The speaker was placed on the wall at a fixed distance of 10cm from the sensor. However, in this experiment, we varied the speaker’s location within the sensing area, ranging from the center of the sensor to near the edge of the sensor.

4.2.2 Data Collection. Data was collected by placing the speaker above seven locations relatively evenly spread out along the edge of the sensor and seven locations near the center of the sensor (Figure 7). At each location, we collected 10 samples for each frequency ranging from 2Hz to 2kHz.

4.2.3 Results. In real-world scenarios, the location of the air-bone vibration source cannot be controlled. Therefore, instead of providing a detailed analysis to compare the signal among each individual location, we focused on the difference between the locations near

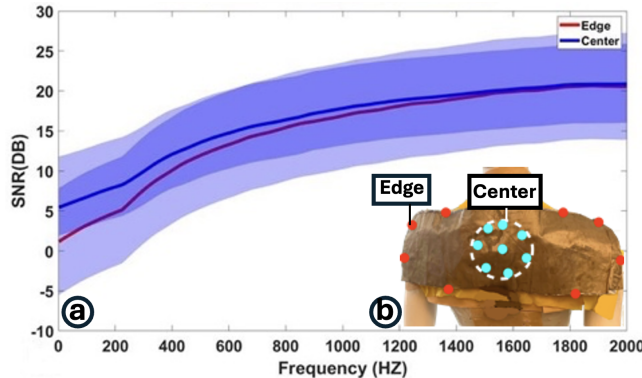


Figure 7: a. Comparison of Sensor Sensitivity Across Different Locations from 0 to 2 kHz. b. Experimental Setup Overview.

the center of the IntelliLining sensor versus the edge of it. We aggregated the sensor data between these two conditions. A t-test suggested no significant effect of location ($p = 0.12$) across the tested locations. However, upon closer examination of the lower range of the spectrum, we observed a noticeable drop in signal strength in the edge condition (2Hz to 800Hz; all $p < 0.05$) (see Figure 7), suggesting potential variations in sensor signals for the same activities occurring at different locations relative to the sensor. This phenomenon is commonly observed in vibration sensors and can likely be addressed using machine learning.

4.3 Effect of Deformation

The inherent stiffness of interlining in garments is designed to provide structural support. However, the fabric sensor is still prone to deformation to accommodate various interlining applications. For instance, sleeve cuffs or collars necessitate their interlining to be deformed into a cylindrical shape. Such deformation could lead to additional strain on the sensor's structure and potentially affect its sensitivity. Therefore, the primary objective of this study was to investigate the impact of static deformation on sensor signals.

4.3.1 Apparatus. To control the deformation of the sensor, the IntelliLining sensor was attached to a cardboard surface coated with artificial skin. The cardboard was then flexed at various angles to induce controlled deformation of the sensor. The experiment used the same sensor with a surface area of 700cm^2 while maintaining the remainder of the speaker setup consistent with previous experiment.

4.3.2 Data Collection. To create the desired deformations, the sensor was incrementally rolled from its initial position (0° or flat) to a fully formed cylinder (360°) at intervals of 90° . This resulted in five different levels of deformation, corresponding to 0° , 90° , 180° , 270° , 360° , each representing the curvature of a circle with radius of 29.6 cm, 14.8 cm, 10 cm, 7.4 cm, starting from 90° (Figure 8). It is noteworthy that our testing focused on deforming the sensor into a curved surface resembling a (partial) cylinder, as this configuration best simulates the way interlinings are deformed within a garment, such as in the case of sleeve cuffs or collars. For each tested frequency, 10 samples were gathered, resulting in a total of 10,000

data points for each replicated sensor at a specific deformation angle. The sensor signals received for each tested frequency were then averaged for data analysis. SNRs were then calculated for data analysis.

4.3.3 Result. Figure 8c shows the result. The IntelliLining sensor showed greater sensitivity without deformation than when deformation occurred. The ANOVA test results confirm a statistically significant difference among the signals ($P < 0.01$ and $F_{4,4173} = 141.92$). This finding suggests that deformation increases the strain of the sensor and changes the effective distance between layers, thus affecting sensor sensitivity. Additionally, we also conducted multiple pairwise tests. The findings from Tukey's HSD test revealed a significant difference between the flat condition and all the other conditions ($p < 0.01$), as well as between the 90° condition and the other conditions of deformation angles. However, beyond the 90° condition, there is no significant difference in the sensitivity of the sensors (all $p > 0.05$). This suggests beyond a certain degree of deformation, the sensor's responsiveness remains relatively constant.

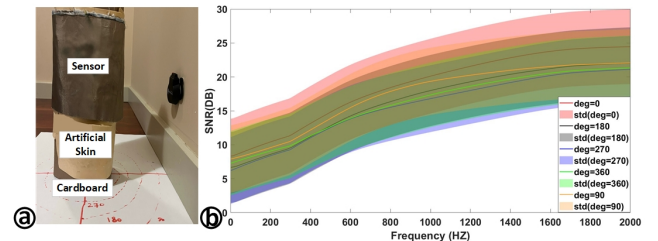


Figure 8: Experiment setup for investigating the effect of sensor deformation. (a) Our setup for controlling the deformation angles. In this image, the sensor has been deformed 360° . (b) SNR of the tested deformation angles shown by frequency.

Upon closer examination of the data, we observed that the sensor maintained good sensitivity even when subjected to a full 360° degree of deformation. This finding is promising and indicates that IntelliLining, when placed on areas such as cuffs and collars, can still effectively detect vibrations. However, it is important to recognize that our study also revealed potential changes in sensor performance when deforming a primarily flat sensor, such as the one on the yoke. These changes may occur due to body movements or different body shapes. However, we anticipate that machine learning can effectively handle such variations in sensing signals, as evidenced by our results in the Evaluation section.

4.4 Airborne vs. Mixed Vibrations

The goal of this study was to evaluate the sensitivity of the sensor in detecting vibrations transmitted solely through the air compared to those transmitted through both air and a surface. These mixed vibrations commonly arise from user activities involving hand interactions with the physical objects, such as chopping or toothbrushing, where both sound and mechanical vibrations are present. Since activities generating purely surface vibrations are relatively uncommon—most user activities produce a mixture of

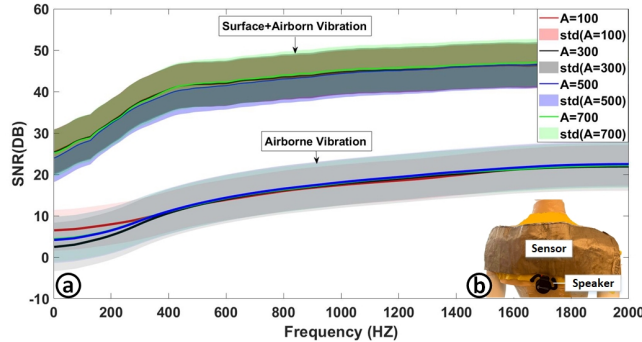


Figure 9: Study setup and result in the mixed surface and airborne vibration condition. (a) SNR shown by frequency in the airborne and mixed conditions. (b) The speaker was placed 15cm below the sensor in surface vibration setup.

airborne and surface vibrations—we chose to exclude pure surface vibrations from our investigation. With airborne vibration data already presented in Section 4.1, our focus shifted to collecting data for the mixed surface and airborne vibration condition.

4.4.1 Apparatus. The experimental setup was similar to the previous study on sensor areas in Section 6.1.1, with the only difference being the placement of the speaker. In this new setup, the speaker was affixed to the artificial skin on the mannequin, positioned 15cm below the sensor (Figure 9). This was to simulate the scenarios, where both surface and airborne vibrations are detected by the sensor.

4.4.2 Data Collection. Like the previous experiment, we gathered 10 samples for every tested frequency, resulting in 10,000 data points for each copy of the sensor in either the airborne or surface vibration condition. We averaged the received sensor signals for each tested frequency for data analysis.

4.4.3 Result. The results are shown in Figure 9. In comparison with the data collected in Section 6.1, we found that the sensor signal in the mixed vibration condition is approximately 25dB higher than in the airborne vibration condition. A one-way ANOVA test revealed a significant difference in signal strength between the two conditions across all sensor areas ($F_{7,7992} = 6404.6$, $p < 0.01$). Although it was anticipated that the signal would exhibit greater strength in the mixed surface and airborne vibration condition, the result offers useful insights into the magnitude of this difference, offering guidance for the development of applications for the interlining sensors. Additionally, this study further confirmed that variations in sensor area did not significantly impact the sensitivity of the sensor at the tested frequencies ($F_{3,3996} = 2.39$ and $P=0.067$).

4.5 Discussion

Through a series of experiments, we demonstrated the feasibility and potential of smart interlining using TENG for capturing a wide spectrum of vibration signals transmitted through the air or a soft and uneven surface. Our results have shown that IntelliLining sensors with a substantial difference in the size of their sensing area

consistently produce similar signal patterns across the tested frequencies. This could greatly reduce the complexity of the system at multiple levels. Nevertheless, events occurring near the edges of the large IntelliLining sensors may exhibit relatively weaker signals than those near the center of the sensor, especially for signal data on the lower end of the spectrum. This suggests that it is more important to include data covering diverse locations within the sensor for activities generating signals at the lower end of the spectrum than for those at the higher end. In addition, our study has revealed that sensor deformation does not significantly affect the sensitivity, especially beyond 90° . This is a promising result for interlining applications, given that the sensors are susceptible to deformation caused by the garment's shape and body movement. Furthermore, our experiment has confirmed the effectiveness of the IntelliLining sensor in capturing airborne vibrations within a short range. This specific characteristic of the vibration sensor is particularly useful for filtering out acoustic sounds in the environment, thereby enhancing the system's robustness in recognizing desired activities.

5 Activity recognition

We conducted a study to measure the accuracy of activity recognition using IntelliLining when integrated into a shirt. Our goal was to measure the accuracy in identifying the three categories of activities described in Section 3.5. We were also interested in determining whether the combined input from the sensor network could enhance recognition accuracy.

5.1 Participants

We recruited ten voluntary participants (28 ± 1.34 years old, 6 female and 4 Male) from our institution. They were asked to wear the prototype shirt outlined in Section 3. This shirt was designed with adjustable straps, allowing it to accommodate participants of varying sizes and body types. We did not secure the sensors tightly to the participants' body at the sensor locations. This choice was made to better simulate real-world usage scenarios. However, a loose fit could introduce sensor noise, which we anticipate can be effectively mitigated by the machine learning model.

5.2 Apparatus

The experimental setup used in this study involved the prototype shirt described in Section 3 (shown in Figure 1). This shirt was designed with five smart interlinings, each serving a distinct purpose: the sleeve cuff, measuring $22.9\text{cm} \times 6.3\text{cm}$ wide; the front placket, measuring $29.5\text{cm} \times 7.5\text{cm}$ wide; the yoke, measuring $46.3\text{cm} \times 15\text{cm}$ wide; the chest pocket, measuring $12\text{cm} \times 12\text{cm}$; and the collar, measuring $42.5\text{cm} \times 2.5\text{cm}$. Data collection from these interlining sensors was conducted using Analog Discovery 2 [1].

5.3 Activities

The experiment included routine activities common in personal and professional life, most of which have been commonly studied in previous research but were only detectable using rigid or non-garment devices [15, 25]. These activities spanned tasks typically carried out using the hand, such as writing on a desk, chopping on a cutting board, clapping hands, and wiping a desk. Additionally, tasks carried out by the mouth, including speaking and snoring,

were also included. Furthermore, activities involving both the hand and mouth, such as brushing teeth, eating bread, drinking a cup of water, and coughing with the hand covering the mouth, were included. Lastly, we also included the activities involving the entire upper body, such as walking and doing crunches (Figure 10). The vibrations from these activities varied in strength and frequency across different users and interlining locations. We are aware that within each category, there are more subtle activities worth investigating, such as recognizing different types of food. We left this investigation for future research.

5.4 Data Collection

Before the experiment started, participants were given several minutes to learn the activities. During the data collection phase, participants were asked to perform the activities in whatever way they felt comfortable. Among the tasks, Writing and Clapping were performed while seated on a chair, whereas Snoring and Crunches were conducted in a lying position. All remaining activities were performed in a standing position. In addition to the 12 tested activities, an idle condition was included (following a common approach [21]), during which data was collected while the participants stood without engaging in any of the tested activities. Participants were allowed to make voluntary body movements, such as adjusting their posture or moving their head, to ensure comfort. Environmental sound, including speech or activity noise from other occupants in the lab, was not controlled, similar to real-world settings.

To mitigate any potential bias, the sequence of all tasks were randomized for each participant. Each trial was recorded for 6 seconds, utilizing the Analog Discovery 2 [1] with a sampling rate of 1024Hz. As a result, every trial contained 6144 data points, and in total, this experiment included $1300 \text{ trials} = 13 \text{ (12 activities + 1 baseline)} * 10 \text{ (repetitions)} * 10 \text{ (participants)}$.

5.5 Machine Learning

To recognize user activities from collected data, we explored both feature-based machine learning and deep learning approaches. This involved several key steps.

First, for both approaches, we expanded the training dataset using time-shifting augmentation, a widely used technique [43]. Each 6-second signal was shifted by 0.5 and 1 second, tripling the training data volume.

In the feature-based approach, signals from five sensors were then concatenated, and 1115 features were extracted using the tsfresh library [10], configured with EfficientFCParameters. These features spanned frequency and time domains, statistical variations, entropy, and lag features (Table 1). A Random Forest model (scikit-learn [34]) with 200 trees and a maximum depth of 30 was trained on this data, balancing accuracy and complexity. Training was conducted on a Windows machine.

For the deep learning approach, augmented signals were normalized with MinMaxScaler and concatenated into sequences. Instead of manual feature extraction, we used a hybrid 1D CNN-LSTM architecture (Figure 11), which automatically learns spatial and temporal representations. This architecture, consisting of convolutional layers with max-pooling and dropout followed by LSTM and dense layers, was implemented in TensorFlow [3]. The model,

trained over 50 epochs with a batch size of 32, used categorical cross-entropy loss and the Adam optimizer. Training and evaluation were conducted on Google Colab with GPU support.

5.6 Result

We present the evaluation results of our system's recognition accuracy, which was assessed using within-user accuracy and cross-user accuracy.

5.6.1 Within-user Accuracy. Within-user accuracy was the measurement of the prediction accuracy where the training and testing data were from the same participant. For each participant, we conducted a ten-fold cross-validation, where one trial of the data was used for testing and the remaining data for training. The overall within-user accuracy was calculated by averaging the results from all the participants. The confusion matrix for the feature-based machine learning approach is shown in Figure 12a. The average accuracy across all activities was 90.02% (STD: 6.7). We found that activities primarily involving hand movements, such as writing, clapping, chopping, and wiping the desk, were accurately classified. Note that within this group, certain activities, like writing and wiping, do not produce distinct audible sounds, yet they still achieved decent accuracy. This highlights the system's capability to recognize subtle vibrations captured by the interlining sensors. Furthermore, our result shows that the system effectively handled variations within the same activity. For instance, even within the same user, clapping was performed with different intensities, and the system was able to accommodate these variations. Note that Coughing exhibited the lowest accuracy (81.3%), often being misclassified as drinking or doing crunches. This misclassification was likely due to the inconsistent and unintentional upper body movements associated with coughing.

In addition, we also conducted a leave-one-sensor-out analysis to understand the importance of the interlining sensors collaboratively contributing to the accurate recognition of these activities. This involved sequentially excluding the data from one sensor at a time, and then training and testing the model using the data from the remaining sensors. This process was repeated for each interlining sensor. Our results showed a decline in the overall accuracy whenever any sensor was omitted. The significance of sensors' locations, in descending order, was: sleeve cuff, collar, front placket, yoke, and chest pocket. When each sensor was individually removed, the corresponding within-user accuracy was: 79.92% for removing the cuff sensor, 82.46% for removing the collar sensor, 84.16% for removing the front placket sensor, 85% for removing the yoke sensor, and 86.72% for removing the chest pocket sensor. These results were reasonable, given the high sensitivity of the interlining sensor on the sleeve cuff to hand movements, which are widely involved in the tested activities, highlighting its crucial role in our system. Notably, the sensor on the chest pocket, despite being the least critical among the sensors, still had a significant impact on accuracy. This indicates that the data obtained from chest movement captured by the pocket sensor also contributed valuable information, particularly in activities such as drinking and crunching. After the removal of the data from the pocket sensor, both activities experienced a nearly 8% accuracy loss.

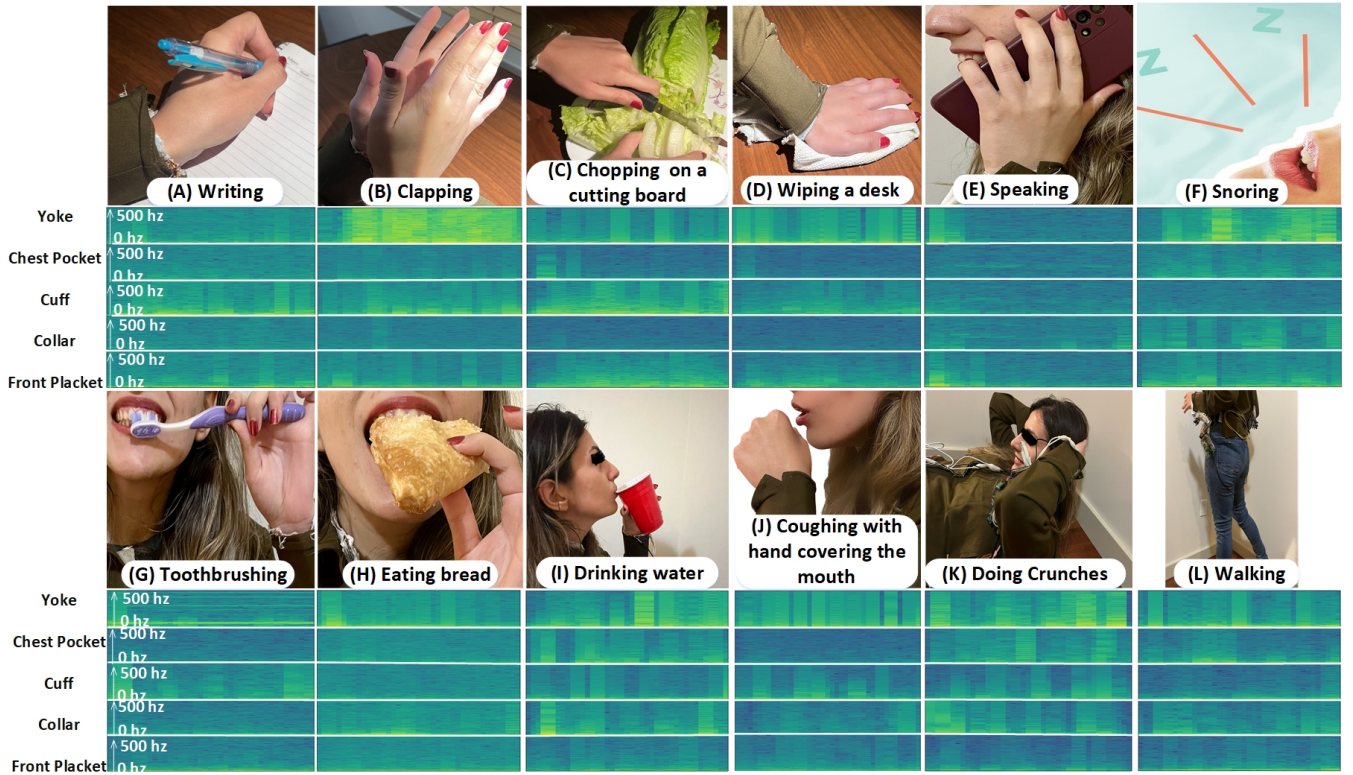


Figure 10: The tested activities with their spectrogram, including the activities involving hand movement, such as writing on a desk, clapping, chopping on a cutting board, wiping a desk (A-D), activities involving mouth movement, such as speaking and snoring (E-F), activities involving both mouth and hand, such as toothbrushing, eating bread, drinking water, coughing with the hand covering the mouth (G-J), and activities involving the entire upper body: doing crunches and walking (K-L).

Category	Extracted Features
Statistical	Absolute energy, absolute Max, sum of changes, Aggregation autocorrelation, entropy, ar coefficient, auto correlation, benford correlation, c3, binned-entropy, complexity, count above mean, count below mean, energy ration by chunk, friedrich coefficients, mass quantilr, kurtosis, variance, time reversal asymmetry, sum values, symmetry values, sum of reaccuring data, sum of reoccuring values, welch density, skewness, sample entropy, rrot mean square, query similiarity count
Frequency Domain	cwt coefficient, fft aggregated, fft coefficient, fourier entropy
Shape features	first location of max, first location of min, duplicate features, duplicate max, duplicate min, last location of max, last location of min, number of peaks, number of cwt peaks

Table 1: The extracted features from our sensor signals

Finally, we explored the accuracy of the deep learning approach. The confusion matrix is shown in Figure 12b. The average within-user accuracy was ~94% which is higher than the average accuracy of ~90% with the feature-based machine learning. Particularly, the deep learning approach improved the within-user accuracy of recognition of the following activities: Wiping a desk (D)(from 86.8% to 94.5%), Snoring(F)(from 86.8% to 91.2%), Coughing (J)(from 81.3% to 90.1%), Crunches (K)(from 84.6% to 91.2%) and Walking (L)(from

85.7% to 92.3%). Most notably, the deep learning technique achieved a 90+% accuracy for all the activities.

5.6.2 Cross-user accuracy. Across-user accuracy measured how well a model worked across different users. We conducted a leave-one-user-out cross-validation by using the data from nine participants for training and the remaining one for testing. The results demonstrated an overall accuracy of 85.5% across all 13 activities.

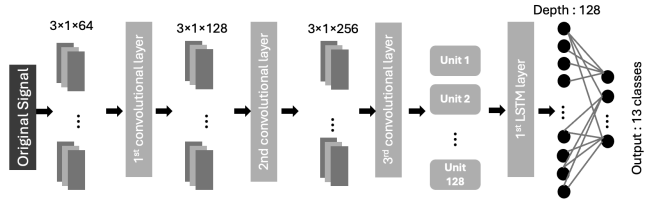


Figure 11: Deep learning network architecture.

Figure 12c provided a detailed confusion matrix for the feature-based machine learning approach. Notably, the accuracy of writing (92.3%) slightly increased in comparison to the within-user accuracy (89%). This suggests that a more diverse training dataset for the writing activity improved the model's ability to recognize writing patterns, even across different users. In contrast, we found a notable drop in accuracy for speaking (89.7%), wiping the desk (79.1%), clapping (81.3%), and toothbrushing (82.4%). The increased variation in vibration patterns observed during these activities suggests there is a greater disparity among different users compared to writing. However, we anticipate that a more extensive training dataset could enhance the model's ability to accurately classify these activities across various users.

Similar to within-user accuracy, we also conducted the leave-one-sensor-out analysis to evaluate the collective contribution of interlining sensors in accurately recognizing various activities. The accuracies corresponding to the removal of the sensor inside the collar, yoke, chest pocket, front placket, and sleeve cuff were found to be 83.52%, 81.8%, 80.23%, 78.7%, and 75.4%, respectively. As these results indicate, in the cross-user scenario, the exclusion of the sleeve cuff sensor also significantly impacted the recognition accuracy, particularly during activities involving the hand, such as writing, wiping, and coughing. In contrast to the within-user scenario, however, in the cross-user setting, the chest pocket sensor demonstrated notably greater importance compared to the collar sensor, as evidenced by the more substantial decline in accuracy upon its removal. This difference was particularly apparent during activities such as coughing, wiping the desk, and toothbrushing. The results of this study offer further evidence to support the combined contribution of the interlining sensors positioned at different locations in handling scenarios involving a diverse range of activities and users.

On the other hand, the deep learning architecture demonstrated an average accuracy of approximately 90%, improving from 86% achieved by the feature-based machine learning approach. The corresponding confusion matrix is presented in Figure 12d. Notably, the deep learning approach scales effectively across users, with all activities reaching a minimum accuracy of around 86%. In contrast, feature-based machine learning yielded lower performance for certain activities, such as Wiping a Desk (D) and Coughing (J), which achieved accuracies of approximately 79% and 78%, respectively.

6 Limitation and Future Work

In this section, we acknowledge the limitations of our study and provide potential future research to address unanswered questions and expand on our finding.

Noise cancellation. Our findings demonstrate that the TENG sensors effectively filter out common ambient noises encountered in everyday environments due to their limited detection range. However, it is anticipated louder noises, such as traffic sounds exceeding 90 dB, may still pose challenges for our current implementation. To mitigate this issue, we propose the incorporation of Adaptive Noise Cancellation (ANC) in our next iteration. This technique would involve one of the interlining sensors serving as the reference source for noise signals. By dynamically adapting and canceling out noise from other sensor inputs, ANC could significantly improve noise filtering capabilities. Importantly, this approach would enable the sensor to continue functioning for activity detection, as it would not be necessary to fully dedicate the sensor to collecting noise data. Instead, allocating a few duty cycles for noise referencing would likely suffice. This approach holds promise for improving the overall effectiveness of our implementation in real-world scenarios.

Device form factor. Our current system implementation requires the use of external devices, such as Analog Discovery 2, for signal capturing and processing. However, looking ahead to a more integrated approach, the development of a fully embedded system is necessary. One promising avenue is the use of widely adopted open-source e-textile toolkits [13], such as the LilyPad. Integrating these toolkits will not only enhance the system's wearability but also facilitate user studies on a broader scale, including a wider range of activities, environments, and users with diverse profiles. This, in turn, will provide more comprehensive insights into the practical application of our interlining sensors.

Improving fabrication for better sensing performance. Optimizing fabrication processes could potentially improve sensing performance. In our work, we fabricated IntelliLining prototypes by sewing multiple layers along the edge. This method was chosen to provide greater freedom of movement for the triboelectric material to bounce between two conductive layers. However, it is important to acknowledge that this approach might not represent the most optimal design, as we did not thoroughly investigate the impact of other fabrication parameters, such as sewing patterns and their location, which could potentially affect signal strength. For our future research, we plan to conduct further investigation to thoroughly evaluate the effects of various fabrication parameters on the sensor's performance.

Sensor durability. In the current implementation of IntelliLining, the decision to utilize PTFE film as the triboelectric material was primarily driven by its cost-effectiveness and flexibility, making it well-suited for prototyping purposes. However, the practical application of PTFE film has revealed its susceptibility to damage due to its fragility. The development of holes in the PTFE film often results in the two conductive layers coming into contact with each other, ultimately leading to short circuits. To address this issue and improve our current implementation, we plan to explore alternative materials, with a specific focus on textile-based triboelectric materials such as Cotton lycra [21]. These materials offer superior durability while retaining efficient electricity generation, thereby mitigating the risk of damage and ensuring consistent sensor performance.

Handle Unintended Activities. In its current implementation, our system addresses unintended activities outside the training dataset by assigning them to an idle class, similar to many existing approaches [25, 33]. However, we recognize that this straightforward

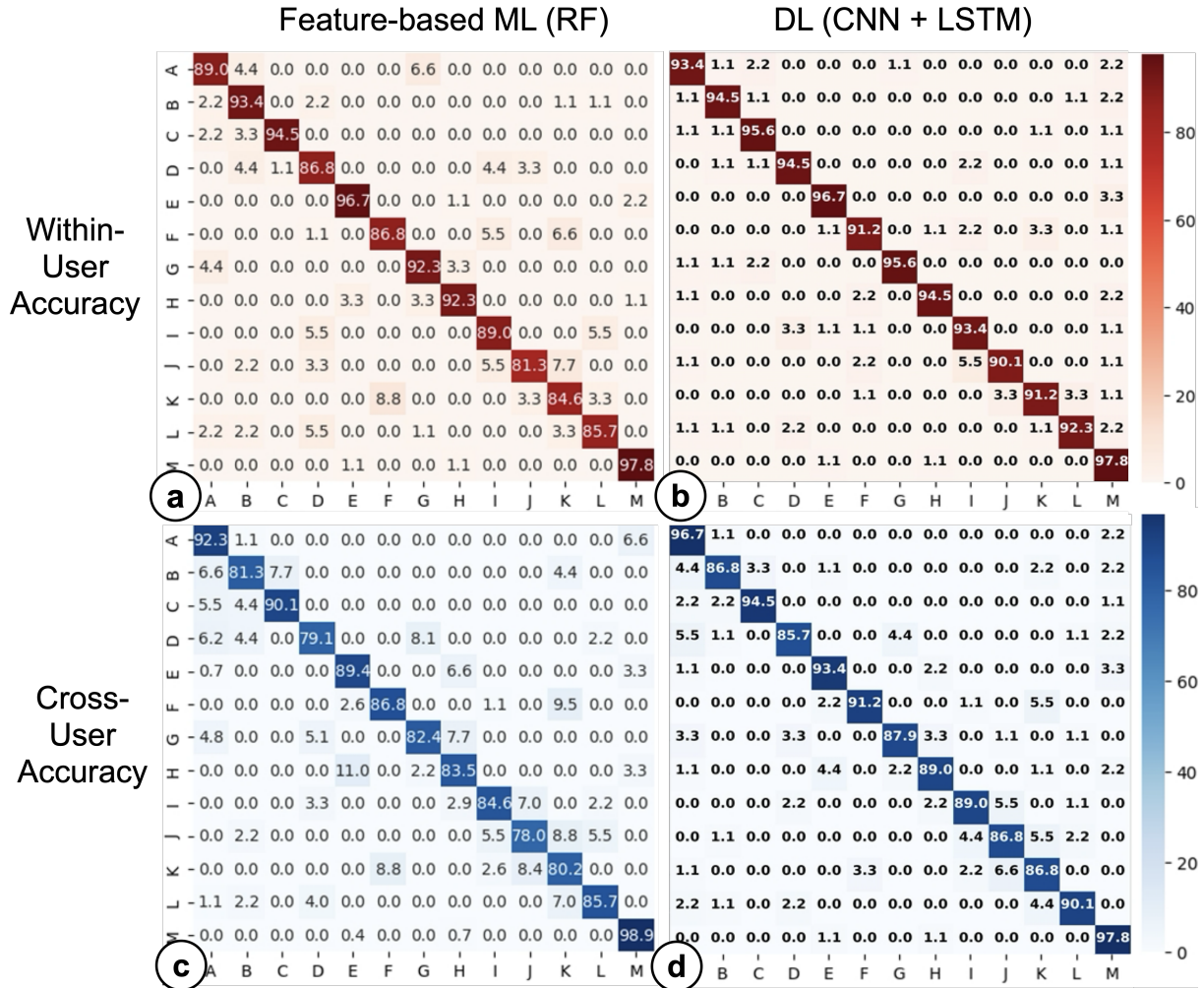


Figure 12: The confusion matrices for (a)within-users accuracy of the feature-based machine learning approach (b) and the deep learning approach and (c), and cross-users accuracy of of the feature-based machine learning approach (d) and the deep learning approach and . The activities include (A) Writing on a desk, (B) Clapping, (C) Chopping on a cutting board, (D) Wiping a desk, (E) Speaking, (F) Snoring, (G) Toothbrushing, (H) Eating bread, (I) Drinking water, (J) Coughing with the hand covering the mouth, (K) Doing crunches, (L) Walking, (M) Idle.

approach has limitations and could be refined to improve its applicability in practical scenarios. For instance, incorporating anomaly detection techniques could provide a more robust solution. Such methods would enable the identification of activities that deviate significantly from the labeled data during recognition, allowing these outliers to be classified as "Idle" to indicate the detection of unintended activities.

7 Conclusion

In this paper, we introduce a new smart garment component—smart interlining. We study the technical feasibility of smart interlining implemented using TENG, a commonly used textile vibration sensor. Through a series of technical experiments, we assess the feasibility of IntelliLining with varying sensing area sizes, deformation, and

the capability to detect surface or airborne vibrations. Additionally, a user evaluation reveals that the recognition accuracy of IntelliLining exceeds 90% across three categories of 12 common activities. Our findings open avenues for future investigations into the practical feasibility of interlining-based sensing in wearable technology, offering a promising direction for advancements in user-friendly and effective smart garment design.

References

- [1] 2023. Analog Discovery 2: 100MS/s USB Oscilloscope, Logic Analyzer and Variable Power Supply. <https://digilent.com/shop/analog-discovery-2-100ms-s-usb-oscilloscope-logic-analyzer-and-variable-power-supply/> Accessed: 2023-08, Digilent.
- [2] Aug 2023. Datasheet of DAEX25 Sound Exciter Pair. <https://www.daytonaudio.com/images/resources/300-375--dayton-audio-daex25-specifications.pdf>

- [3] Martin Abadi, Ashish Agarwal, Paul Barham, Eugene Brevdo, Zhifeng Chen, Craig Citro, Greg S. Corrado, Andy Davis, Jeffrey Dean, Matthieu Devin, Sanjay Ghemawat, Ian Goodfellow, Andrew Harp, Geoffrey Irving, Michael Isard, Yangqing Jia, Rafal Jozefowicz, Lukasz Kaiser, Manjunath Kudlur, Josh Levenberg, Dan Mané, Rajat Monga, Sherry Moore, Derek Murray, Chris Olah, Mike Schuster, Jonathon Shlens, Benoit Steiner, Ilya Sutskever, Kunal Talwar, Paul Tucker, Vincent Vanhoucke, Vijay Vasudevan, Fernanda Viégas, Oriol Vinyals, Pete Warden, Martin Wattenberg, Martin Wicke, Yuan Yu, and Xiaoqiang Zheng. 2015. TensorFlow: Large-Scale Machine Learning on Heterogeneous Systems. <http://tensorflow.org/> Software available from tensorflow.org.
- [4] Amazon Amazon. 2023. Bulk Oil Slick Sheet laboratory grade PTFE roll solvent resistant ... <https://www.amazon.com/Oil-Slick-Labratory-Resistant-Alternative/dp/B01D0RB0UI>
- [5] Amazon Amazon. 2023. Mission darkness titanrf faraday fabric kit 1 yard // military grade conductive material blocks RF signals (WIFI, cell, Bluetooth, RFID, EMF) // 44" W X 36" fabric + 36" Tape: Amazon.ca: Industrial & Scientific. https://www.amazon.ca/dp/B01M294MGK?ref=ppx_yo2ov_dt_b_product_details&th=1
- [6] Nivedita Arora, Steven L. Zhang, Fereshteh Shahmiri, Diego Osorio, Yi-Cheng Wang, Mohit Gupta, Zhengjun Wang, Thad Starner, Zhong Lin Wang, and Gregory D. Abowd. 2018. SATURN: A Thin and Flexible Self-powered Microphone Leveraging Triboelectric Nanogenerator. *Proceedings of the ACM on Interactive, Mobile, Wearable and Ubiquitous Technologies* 2, 2 (2018), 1–28. <https://doi.org/10.1145/3214263>
- [7] Ronald J. Baker. 1987. *Clinical Measurement of Speech and Voice*. College-Hill Press, Boston, MA. 528 pages. <https://doi.org/10.1288/00005537-198808000-00028>
- [8] Hymalai Bello, Bo Zhou, Sungju Suh, and Paul Lukowicz. 2021. MoCapaci: Posture and Gesture Detection in Loose Garments Using Textile Cables as Capacitive Antennas. In *Proceedings of the 2021 ACM International Symposium on Wearable Computers (Virtual, USA) (ISWC '21)*. Association for Computing Machinery, New York, NY, USA, 78–83. <https://doi.org/10.1145/3460421.3480418>
- [9] Youngsu Cha, Hojoon Kim, and Doik Kim. 2018. Flexible piezoelectric sensor-based gait recognition. *Sensors* 18, 2 (2018), 468. <https://doi.org/10.3390/s18020468>
- [10] Maximilian Christ, Nils Braun, Julius Neuffer, and Andreas W. Kempa-Liehr. 2023. Tsfresh. <https://tsfresh.readthedocs.io/en/latest/index.html>
- [11] Artem Dementyev, Tomás Vega Gálvez, and Alex Olwal. 2019. SensorSnaps: Integrating Wireless Sensor Nodes into Fabric Snap Fasteners for Textile Interfaces. In *Proceedings of the 32nd Annual ACM Symposium on User Interface Software and Technology* (New Orleans, LA, USA) (UIST '19). Association for Computing Machinery, New York, NY, USA, 17–28. <https://doi.org/10.1145/3332165.3347913>
- [12] T. N. H. Doan, V. K. Nguyen, and N. C. Dao. 2016. A Textile Antenna for Wearable Applications Using RFID Technology. In *Proceedings of the 10th International Conference on Ubiquitous Information Management and Communication (IMCOM '16)*. Association for Computing Machinery, New York, NY, USA, 1–4. <https://doi.org/10.1145/2857546.2857621>
- [13] E-textile. n.d.. Toolkits. <https://www.sparkfun.com/categories/204> Accessed: 2025-02-11.
- [14] Feng-Ru Fan, Zhong-Qun Tian, and Zhong Lin Wang. 2012. Flexible triboelectric generator. *Nano Energy* 1, 2 (2012), 328–334. <https://doi.org/10.1016/j.nanoen.2012.01.004>
- [15] Biyi Fang, Nicholas D. Lane, Mi Zhang, and Fahim Kawsar. 2016. HeadScan: A Wearable System for Radio-Based Sensing of Head and Mouth-Related Activities. In *2016 15th ACM/IEEE International Conference on Information Processing in Sensor Networks (IPSN)*. 1–12. <https://doi.org/10.1109/IPSN.2016.7460677>
- [16] F. Gemperle, C. Kasabach, J. Stivoric, M. Bauer, and R. Martin. 1998. Design for wearability. In *Digest of Papers Second International Symposium on Wearable Computers (Cat. No.98EX215)*. 116–122. <https://doi.org/10.1109/ISWC.1998.729537>
- [17] Holger Harm, Oliver Amft, Daniel Roggen, and Gerhard Tröster. 2010. Smash: A distributed sensing and processing garment for the classification of upper body postures. In *3rd International ICST Conference on Body Area Networks*.
- [18] Hui Huang, Xian Li, Si Liu, Shihyan Hu, and Ye Sun. 2018. TriboMotion: A Self-Powered Triboelectric Motion Sensor in Wearable Internet of Things for Human Activity Recognition and Energy Harvesting. *IEEE Internet of Things Journal* 5, 6 (2018), 4441–4453. <https://doi.org/10.1109/JIOT.2018.2817841>
- [19] Pyeong-Gook Jung, Gukchan Lim, Seonghyok Kim, and Kyoungchul Kong. 2015. A wearable gesture recognition device for detecting muscular activities based on air-pressure sensors. *IEEE Transactions on Industrial Informatics* 11, 2 (2015), 485–494. <https://doi.org/10.1109/TII.2014.2346799>
- [20] Aftab Khan, Sebastian Mellor, Eugen Berlin, Robin Thompson, Roisin McNaney, Patrick Olivier, and Thomas Plötz. 2015. Beyond activity recognition: skill assessment from accelerometer data. In *Proceedings of the 2015 ACM International Joint Conference on Pervasive and Ubiquitous Computing (Osaka, Japan) (UbiComp '15)*. Association for Computing Machinery, New York, NY, USA, 1155–1166. <https://doi.org/10.1145/2750858.2807534>
- [21] Ali Kiaghadi, Morgan Baima, Jeremy Gummesson, Trisha Andrew, and Deepak Ganeshan. 2018. Fabric as a Sensor: Towards unobtrusive sensing of human behavior with triboelectric textiles. *SenSys 2018 - Proceedings of the 16th Conference on Embedded Networked Sensor Systems* (2018), 199–210. <https://doi.org/10.1145/3274783.3274845>
- [22] Bonhak Koo, Ngoc Tram Nguyen, and Jooyong Kim. 2023. Identification and Classification of Human Body Exercises on Smart Textile Bands by Combining Decision Tree and Convolutional Neural Networks. *Sensors* 23, 13 (2023). <https://doi.org/10.3390/s23136223>
- [23] Yuya Koyama, Michiko Nishiyama, and Kazuhiro Watanabe. 2018. Physical activity recognition using hetero-core optical fiber sensors embedded in a smart clothing. In *2018 IEEE 7th Global Conference on Consumer Electronics (GCCE)*. IEEE, 71–72. <https://doi.org/10.1109/GCCE.2018.8574738>
- [24] Pin-Sung Ku, Jun Gong, Te-Yen Wu, Yixin Wei, Yiwen Tang, Barrett Ens, and Xing-Dong Yang. 2020. Zipplo: The Design and Implementation of An Interactive Zipper. In *Proceedings of the 2020 CHI Conference on Human Factors in Computing Systems (Honolulu, HI, USA) (CHI '20)*. Association for Computing Machinery, New York, NY, USA, 1–13. <https://doi.org/10.1145/3313831.3376756>
- [25] Gierad Laput, Robert Xiao, and Chris Harrison. 2016. ViBand: High-fidelity bio-acoustic sensing using commodity smartwatch accelerometers. *UIST 2016 - Proceedings of the 29th Annual Symposium on User Interface Software and Technology* (2016), 321–333. <https://doi.org/10.1145/2984511.2984582>
- [26] Jiaron Li, Zihan Wang, Zihao Zhao, Yuchao Jin, Jihong Yin, Shao-Lun Huang, and Jiyu Wang. 2021. TriboGait: A deep learning enabled triboelectric gait sensor system for human activity recognition and individual identification. In *Adjunct Proceedings of the 2021 ACM International Joint Conference on Pervasive and Ubiquitous Computing and Proceedings of the 2021 ACM International Symposium on Wearable Computers*. <https://api.semanticscholar.org/CorpusID:237619074>
- [27] Qi Lin, Shuhua Peng, Yuezhong Wu, Jun Liu, Wen Hu, Mahbub Hassan, Aruna Seneviratne, and Chun H. Wang. 2020. E-jacket: Posture detection with loose-fitting garment using a novel strain sensor. In *2020 19th ACM/IEEE International Conference on Information Processing in Sensor Networks (IPSN)*. IEEE, 49–60.
- [28] Qi Lin, Shuhua Peng, Yuezhong Wu, Jun Liu, Hong Jia, Wen Hu, Mahbub Hassan, Aruna Seneviratne, and Chun H. Wang. 2023. Subject-Adaptive Loose-fitting Smart Garment Platform for Human Activity Recognition. *ACM Transactions on Sensor Networks* 19, 4 (2023). <https://doi.org/10.1145/3584986>
- [29] Gabriel Loke, Turak Khudiyev, Brian Wang, Stephanie Fu, Syamantak Payra, Yorai Shaoul, Johnny Fung, Ioannis Chatziveroglou, Pin-Wen Chou, Itamar Chinn, et al. 2021. Digital electronics in fibres enable fabric-based machine-learning inference. *Nature communications* 12, 1 (2021), 3317.
- [30] Hua Ma and Junichi Yamaoka. 2022. SenSequins: Smart Textile Using 3D Printed Conductive Sequins. In *The 35th Annual ACM Symposium on User Interface Software and Technology, UIST 2022, Bend, OR, USA, 29 October 2022 - 2 November 2022*. Maneesh Agrawala, Jacob O. Wobbrock, Eytan Adar, and Vidya Setlur (Eds.). ACM, 85:1–85:13. <https://doi.org/10.1145/3526113.3545688>
- [31] Alex Olwal, Thad Starner, and Gowa Mainini. 2020. E-Textile Microinteractions: Augmenting Twist with Flick, Slide and Grasp Gestures for Soft Electronics. In *Proceedings of the 2020 CHI Conference on Human Factors in Computing Systems (Honolulu, HI, USA) (CHI '20)*. Association for Computing Machinery, New York, NY, USA, 1–13. <https://doi.org/10.1145/3313831.3376236>
- [32] Patrick Parzer, Florian Perteneder, Kathrin Probst, Christian Rendl, Joanne Leong, Sarah Schuetz, Anita Vogl, Reinhard Schwoedauer, Martin Kaltenbrunner, Siegfried Bauer, and Michael Haller. 2018. RESI: A Highly Flexible, Pressure-Sensitive, Imperceptible Textile Interface Based on Resistive Yarns. In *Proceedings of the 31st Annual ACM Symposium on User Interface Software and Technology (UIST '18)*. Association for Computing Machinery, New York, NY, USA, 745–756. <https://doi.org/10.1145/3242587.3242664>
- [33] Patrick Parzer, Adwait Sharma, Anita Vogl, Jürgen Steinle, Alex Olwal, and Michael Haller. 2017. SmartSleeve: Real-time Sensing of Surface and Deformation Gestures on Flexible, Interactive Textiles, using a Hybrid Gesture Detection Pipeline. In *Proceedings of the 30th Annual ACM Symposium on User Interface Software and Technology (UIST '17)*. Association for Computing Machinery, New York, NY, USA, 565–577. <https://doi.org/10.1145/3126594.3126652>
- [34] F. Pedregosa, G. Varoquaux, A. Gramfort, V. Michel, B. Thirion, O. Grisel, M. Blondel, P. Prettenhofer, R. Weiss, V. Dubourg, J. Vanderplas, A. Passos, D. Cournapeau, M. Brucher, M. Perrot, and E. Duchesnay. 2011. Scikit-learn: Machine Learning in Python. *Journal of Machine Learning Research* 12 (2011), 2825–2830.
- [35] Ivan Poupyrev, Nan-Wei Gong, Shihui Fukuhara, Mustafa Emre Karagozler, Carsten Schwesig, and Karen E. Robinson. 2016. Project Jacquard: Interactive Digital Textiles at Scale. In *Proceedings of the 2016 CHI Conference on Human Factors in Computing Systems (San Jose, California, USA) (CHI '16)*. Association for Computing Machinery, New York, NY, USA, 4216–4227. <https://doi.org/10.1145/2858036.2858176>
- [36] Rajarajan Ramalingame, Rim Baroilo, Xupeng Li, Giuseppe Sanseverino, Dominik Krumm, Stephan Odenwald, and Olfa Kanoun. 2021. Wearable smart band for American sign language recognition with polymer carbon nanocomposite-based pressure sensors. *IEEE Sensors Letters* 5, 6 (2021), 1–4.
- [37] Olivia G Ruston, Adwait Sharma, and Mike Fraser. 2024. SeamSleeve: Robust Arm Movement Sensing through Powered Stitching. In *Proceedings of the 2024 ACM Designing Interactive Systems Conference (IT University of Copenhagen, Denmark) (DIS '24)*. Association for Computing Machinery, New York, NY, USA, 1134–1147. <https://doi.org/10.1145/3643834.3660726>

- [38] Teddy Seyed, James Devine, Joe Finney, Michal Moskal, Peli de Halleux, Steve Hodges, Thomas Ball, and Asta Roseway. 2021. Rethinking the Runway: Using Avant-Garde Fashion To Design a System for Wearables. In *Proceedings of the 2021 CHI Conference on Human Factors in Computing Systems (CHI '21)*. ACM, 1–15. <https://www.microsoft.com/en-us/research/publication/rethinking-the-runway-using-avant-garde-fashion-to-design-a-system-for-wearables/>
- [39] Fereshteh Shahmiri, Chaoyu Chen, Anandghan Waghmare, Dingtian Zhang, Shivan Mittal, Steven L. Zhang, Yi-Cheng Wang, Zhong Lin Wang, Thad E. Starner, and Gregory D. Abowd. 2019. Serpentine: A Self-Powered Reversibly Deformable Cord Sensor for Human Input. In *Proceedings of the 2019 CHI Conference on Human Factors in Computing Systems (Glasgow, Scotland UK) (CHI '19)*. Association for Computing Machinery, New York, NY, USA, 1–14. <https://doi.org/10.1145/3290605.3300775>
- [40] Sungtae Shin, Han Ul Yoon, and Byungseok Yoo. 2021. Hand gesture recognition using EGaIn-silicone soft sensors. *Sensors* 21, 9 (2021), 3204.
- [41] Kumar Shrestha, Gagan Bahadur Pradhan, Trilochan Bhatta, Sudeep Sharma, Sanghyun Lee, Hyesu Song, Seonghoon Jeong, and Jae Y. Park. 2023. Intermediate nanofibrous charge trapping layer-based wearable triboelectric self-powered sensor for human activity recognition and user identification. *Nano Energy* 108 (2023), 108180. <https://doi.org/10.1016/j.nanoen.2023.108180>
- [42] Sophie Skach, Rebecca Stewart, and Patrick G. T. Healey. 2018. Smart Arse: Posture Classification with Textile Sensors in Trousers. In *Proceedings of the 20th ACM International Conference on Multimodal Interaction (Boulder, CO, USA) (ICMI '18)*. Association for Computing Machinery, New York, NY, USA, 116–124. <https://doi.org/10.1145/3242969.3242977>
- [43] Qingsong Wen, Liang Sun, Fan Yang, Xiaomin Song, Jingkun Gao, Xue Wang, and Huan Xu. 2021. Time Series Data Augmentation for Deep Learning: A Survey. *IJCAI International Joint Conference on Artificial Intelligence* (2021), 4653–4660. [https://doi.org/10.24963/ijcai.2021/631 arXiv:2002.12478](https://doi.org/10.24963/ijcai.2021/631)
- [44] Te-Yen Wu, Zheer Xu, Xing-Dong Yang, Steve Hodges, and Teddy Seyed. 2021. Project Tasca: Enabling Touch and Contextual Interactions with a Pocket-based Textile Sensor. In *Proceedings of the 2021 CHI Conference on Human Factors in Computing Systems (Yokohama, Japan) (CHI '21)*. Association for Computing Machinery, New York, NY, USA, Article 4, 13 pages. <https://doi.org/10.1145/3411764.3445712>
- [45] Yao Xiong, Ziwei Huo, Jintao Zhang, Yang Liu, Dewu Yue, Nuo Xu, Rui Gu, Liang Wei, Lin Luo, Mingxia Chen, Chao Liu, Zhong Lin Wang, and Qijun Sun. 2024. Triboelectric in-sensor deep learning for self-powered gesture recognition toward multifunctional rescue tasks. *Nano Energy* 124 (2024), 109465. <https://doi.org/10.1016/j.nanoen.2024.109465>
- [46] Haifeng Xu, Renhai Feng, and Weikang Zhang. 2023. C-DTW for Human Action Recognition Based on Nanogenerator. *Sensors* 23, 16 (2023). <https://doi.org/10.3390/s23167230>
- [47] Ran Xu, Fangyuan Luo, Zhiyuan Zhu, Mintong Li, and Bin Chen. 2022. Flexible Wide-Range Triboelectric Sensor for Physiological Signal Monitoring and Human Motion Recognition. *ACS Applied Electronic Materials* 4, 8 (2022), 4051–4060. [https://doi.org/10.1021/acsaelm.2c00681 arXiv:https://doi.org/10.1021/acsaelm.2c00681](https://doi.org/10.1021/acsaelm.2c00681)
- [48] Lixia Yan, Yajun Mi, Yin Lu, Qinghao Qin, Xueqing Wang, Jiajing Meng, Fei Liu, Ning Wang, and Xia Cao. 2022. Weaved piezoresistive triboelectric nanogenerator for human motion monitoring and gesture recognition. *Nano Energy* 96 (2022), 107135. <https://doi.org/10.1016/j.nanoen.2022.107135>
- [49] Tianhong Catherine Yu, Manru Zhang, Peter He, Chi-Jung Lee, Cassidy Cheesman, Saif Mahmud, Ruidong Zhang, François Guimbretière, and Cheng Zhang. 2024. SeamPose: Repurposing Seams as Capacitive Sensors in a Shirt for Upper-Body Pose Tracking. [arXiv:2406.11645 \[cs.HC\]](https://arxiv.org/abs/2406.11645) <https://arxiv.org/abs/2406.11645>
- [50] Clint Zeagler. 2017. Where to Wear It: Functional, Technical, and Social Considerations in on-Body Location for Wearable Technology 20 Years of Designing for Wearability. In *Proceedings of the 2017 ACM International Symposium on Wearable Computers (Maui, Hawaii) (ISWC '17)*. Association for Computing Machinery, New York, NY, USA, 150–157. <https://doi.org/10.1145/3123021.3123042>
- [51] Yuanming Zeng, Huijing Xiang, Ning Zheng, Xia Cao, Ning Wang, and Zhong Lin Wang. 2022. Flexible triboelectric nanogenerator for human motion tracking and gesture recognition. *Nano Energy* 91 (2022), 106601. <https://doi.org/10.1016/j.nanoen.2021.106601>
- [52] Quan Zhang, Tao Jin, Jianguo Cai, Liang Xu, Tianyi He, Tianhong Wang, Yingzhong Tian, Long Li, Yan Peng, and Chengkuo Lee. 2022. Wearable Triboelectric Sensors Enabled Gait Analysis and Waist Motion Capture for IoT-Based Smart Healthcare Applications. *Advanced Science* 9, 4 (2022), 2103694. <https://doi.org/10.1002/advs.202103694 arXiv:https://onlinelibrary.wiley.com/doi/pdf/10.1002/advs.202103694>
- [53] Qian Zhang and Chi Wai Kan. 2018. A review of fusible interlinings usage in garment manufacture. *Polymers* 10, 11 (2018), 1–32. <https://doi.org/10.3390/polym10111230>
- [54] Bo Zhou, Daniel Geissler, Marc Faulhaber, Clara Elisabeth Gleiss, Esther Friederike Zahn, Lala Shakti Swarup Ray, David Gamarra, Vitor Fortes Rey, SungHo Suh, Sizhen Bian, Gesche Joost, and Paul Lukowicz. 2023. MoCaPose: Motion Capturing with Textile-integrated Capacitive Sensors in Loose-fitting Smart Garments. *Proceedings of the ACM on Interactive, Mobile, Wearable and Ubiquitous Technologies* 7, 1 (2023), 1–40. <https://doi.org/10.1145/3580883>